

Recent Development of Si Chemical Dry Etching Technologies

Toshio Hayashi*

Plasma Nano Technology Research Center, Nagoya University, 464-8603, Japan

Abstract

Chemical dry etching in wafer processing was innovated and developed in 1976 using CF_4/O_2 downflow plasma for poly-Si etching. Thereafter, many researchers developed and reported various chemical dry etching methods.

Advanced Si chemical dry etching technology was developed in 2010, using N_2 downflow plasma and NF_3 flowing to the downflow plasma area. The etchant production mechanism for this technology was explained by us.

In these technologies, the plasma source is necessary to produce the etchants (F for Si etching and $HF+NH_3$ for SiO_2 etching).

Recently, a novel Si chemical dry etching technology was innovated and developed by us without plasma source, in which F atoms generated in $F_2+NO \rightarrow F+FNO$ reaction are used for Si etching in the pressure range of 100 to 1000 Pa. The etch rate at room temperature is more than 5000 nm/min, and is dependent on the flow rate and on the distance between the gas mixing point and the wafer position. Increasing the substrate temperature, the minimum etch rate was obtained at 60°C. Over this temperature, the etch rate increased again with increase of the substrate temperature. In the lower temperature region, the chemisorbed layer may be formed and the chemical reaction may be enhanced in this condensed layer. Increasing the temperature, this chemisorbed layer disappears around 60°C. Over this temperature, the surface reaction mainly takes place according to Arrhenius equation.

Keywords: Wafer processing; Dry etching

Introduction

Chemical dry etching (CDE) in wafer processing was first developed by Horiike and Shibagaki [1], using CF_4/O_2 downflow plasma for poly-Si etching, to prevent the degradation of the electrical properties of integrated circuits (ICs) due to the bombardment of charged particles. Thereafter, many researchers developed and reported various chemical dry etching methods [2-11]. Mogab et al. [2] reported the O_2 addition effect in CF_4/O_2 radial flow reactive plasma, in which the maximum Si etch rate was obtained at an O_2 mixing ratio of 15%. A similar phenomenon was observed in a planar capacitive coupled plasma reactor [12]. Flamm et al. [4] derived the regression equation of the Si etch rate observing the chemiluminescence from SiF_3^+ on the Si wafer and the etch rate as a function of the wafer temperature, and also showed that the reaction probability of Si with F was 0.00168 at room temperature. Ninomiya et al. [13] reported that the reaction probability of Si with F was 0.1 at 300 K by gas-phase titration method under careful treatment, avoiding surface oxidation by the ambient. Energetic beam induced XeF_2 etching of Si was investigated by Coburn and Winters [14]. In this report, it was also suggested that the etch rate of Si by XeF_2 gas without beam irradiation was 0.5-0.7 nm/min (at flow rate of $XeF_2=2 \times 10^{15}$ mol/s). The O_2 addition effect in the planar capacitive coupled plasma reactor was clearly explained observing the negative ions emerged from etched Si surface [15]. In this experiment, it was confirmed that the etch rate decrease above the 15% O_2 mixing ratio was mainly due to surface oxidation, because the C_2F_4 negative ion current observed by a mass spectrometer was approximately constant. C_2F_4 molecules are generally formed on the wall surface and released from the surface, because C_2F_4 molecule is very stable and $C_2F_4^-$ ion is formed by thermal electron attachment with the energy of 0.5 eV in the sheath region. In the O_2 mixing ratio lower than 15%, the etched surface was covered with C_xF_y film. At around the maximum etching rate region, C_xF_y film was removed effectively by O atoms and ions, and therefore, F atoms might be consumed by reaction with Si. Further increasing O_2 concentration, the etched surface was partially covered with SiO_x and F consumption decreased. This mechanism leads to the distinct maximum of Si etch rate and F concentration. Therefore, it is

supposed that the similar phenomenon takes place on the Si etched surface in the CF_4/O_2 radial flow reactive plasma.

Thus, chemical dry etching technologies have been studied and developed, but have not been used in wafer fabrication as one of the major etching technologies, because the etch rate cannot be readily controlled, and/or no anisotropic etching profile is obtained. However, this technology turns into a very important one because the removal of damaged Si layer around the gate electrode and residual oxide layer after gate oxide are strongly required in the ultrafine pattern fabrication with a half pitch lower than 45 nm. In these process, slow etch rate is required in order to control the etched depth of around 10 nm, which is damaged by a prior reactive ion etching [16-18], or remains in a prior oxide etching.

CDE Technologies with Long Life Time Plasma Source

The plasma source is constituted by quartz or aluminum oxide tube for these remote plasma sources. Quartz tube is preferably used because recombination of produced hydrogen atoms [19] and fluorine atoms on the quartz tube inner wall is relatively lower. However, when fluorine-containing compound is fed and decomposed in the discharge area, the quartz tube itself is eroded by fluorine containing plasma and has to be replaced with a new one after several hundred batches. If the fluorine containing etchants are produced outside the remote plasma source, the erosion of the plasma source is considerably reduced and the lifetime of the source material becomes longer owing to the reduction in the extent of fluorine erosion.

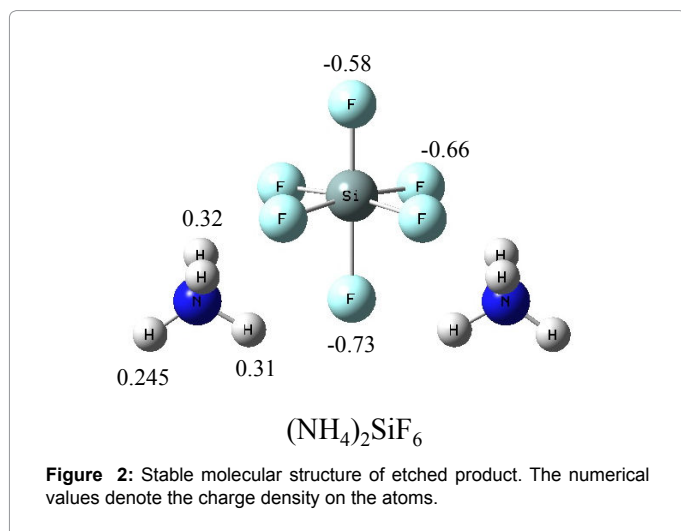
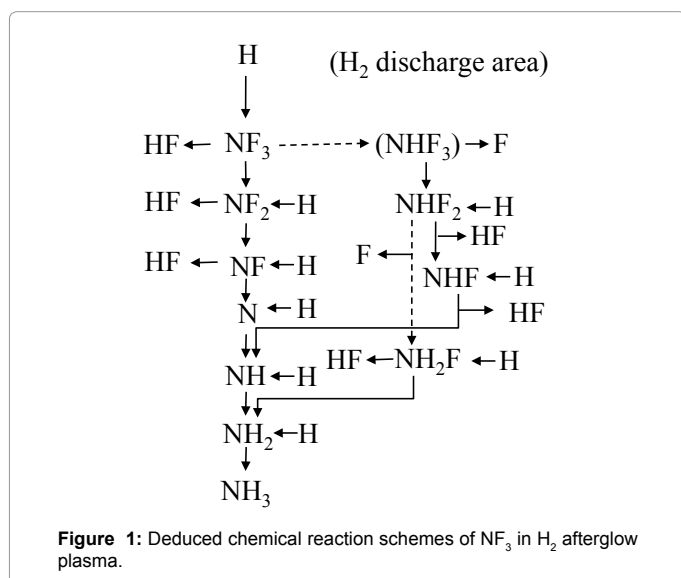
*Corresponding author: Toshio Hayashi, Plasma Nano Technology Research Center, Nagoya University, 464-8603, Japan, E-mail: hayashi@plasma.engg.nagoya-u.ac.jp

Received August 27, 2012; Accepted October 10, 2012; Published October 20, 2012

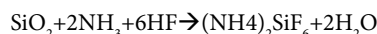
Citation: Hayashi T (2012) Recent Development of Si Chemical Dry Etching Technologies. J Nanomed Nanotechnol S15:001. doi:10.4172/2157-7439.S15-001

Copyright: © 2012 Hayashi T. This is an open-access article distributed under the terms of the Creative Commons Attribution License, which permits unrestricted use, distribution, and reproduction in any medium, provided the original author and source are credited.

Chemical dry etching technology for native oxide removal by flowing NF_3 to H_2+H_2O down flow plasma was first developed by Kikuchi et al. [20,21], to avoid damage to the quartz tube by plasma irradiation. In this process, NF_3 is not decomposed in the plasma source. However, it is thought that the oxide layer is also removed through a similar etching mechanism in the NF_3/NH_3 down flow plasma on the wafer [8]. Oxide layer removal can also be carried out using H_2 , N_2+H_2 or NH_3 down flow plasma and NF_3 flow without decomposition [22]. In these down flow plasmas, hot H atoms initiate the reaction with NF_3 in the down flow area, and then successive reactions take place between H atoms and NF_x ($x=1-2$) [23]. Finally, HF and NH_3 are produced and adsorbed on the wafer surface, proceeding to condensed phase on the wafer surface. In this condensed phase, a sort of ammonium fluoride etching in the liquid phase takes place. It was reported that the etch rate of the chemical dry etching method by flowing to the H_2 , N_2+H_2 , or NH_3 down flow plasma was 1 to 10 nm/min at the room temperature, not depending on the distance between the NF_3 flow position and the wafer stage [22]. These processes are very useful to remove thin oxide layer (10 to 20 nm) for the etching around the gate electrode without the plasma damage.



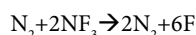
The reaction mechanism for the thin oxide layer removal using H_2 downflow plasma and flowing NF_3 into this downflow plasma at around 500 Pa was clarified by us [23], in which backward flow of NF_3 does not take place owing to viscous flow and F atom is not generated in the plasma source. The total reaction scheme is summarized and illustrated in Figure 1. The solid line shows the main reaction routes and the dashed line shows the minor reaction routes. Some of the reactions depicted in this figure also take place at the surface, because a strong hydrogen bond is formed between the HF and NH_3 produced and the boiling point of this complex molecule exceeds 500 K [24]. Finally, HF and NH_3 are formed and adsorbed on the wafer surface, on which a condensed phase is formed, so that a type of ammonium fluoride etching in the liquid phase takes place. Therefore, experimentally, by decreasing wafer temperature, etch rate increases, depending on temperature. Figure 2 shows the calculated molecular structure of $(NH_4)_2SiF_6$ formed on the SiO_2 surface through the reaction



This complex molecule with two NH_4 groups on the same side is more stable than that with two NH_4 groups on opposite sides to each other, because the coulomb interaction in NH_4-F-NH_4 takes place and stabilizes the molecule. This complex molecule decomposes with an increase in the wafer temperature up to 373 K to release SiF_4 and the white powder remains on the wafer surface, which was deduced as $FH-NH_3-HF$ (coordinate bonded H of HF with N of NH_3) [8]. However, the total cohesive energy (hydrogen bond energy) between two HF and NH_3 molecules is -0.606 eV, which is lower than -0.663 eV of the hydrogen bond energy between HF and NH_3 molecules in B3LYP/6-31+G(d,p) level. This implies that the white powder is not composed of only $FH-NH_3-HF$ and should rather be a huge molecule composed of $(NH_4F)_n$. It was found from the molecular orbital calculation that the white powder was mainly composed of stratified $n(NH_4F)_3$ with a C_3 symmetry axis [23].

A Si etching technology using NF_3 flow into N_2 down flow plasma was found by Tajima and Takahashi [25], at the distance of 20-40 cm apart from the edge of the N_2 plasma source. They reported that the etch rate strongly depended on the etching conditions of the NF_3 and N_2 flow rates at the pressure of 100 to 500 Pa, by applying 2.45 GHz microwave power of 1-2 kW. In their report, the etch rate was especially dependent on the N_2 flow rate ratio at the distance of 40 cm; Si was not etched under a condition of the N_2 and NF_3 flow rates of 0.5 and 1 SLM, and increasing the N_2 flow rate to 1 SLM Si was etched. This means that backward flow of NF_3 does not take place (owing to viscous flow). This etch rate dependence on the N_2 flow rate ratio is very useful to remove the damaged Si layer of approximately 10 nm around gate electrode [16-18], where clean removing the damaged layer without any etched residues is required, and is also to be controllable within 1 to 2 minutes by changing the N_2 flow rate ratio.

Figure 3 shows a schematic diagram of the reaction chamber, in which NF_3 is fed 20-40 cm from the edge of the discharge area at pressures of 100-500 Pa [26]. Under this condition, NF_3 is fed into the downflow area without decomposition and reacts with activated N atoms, and/or activated N_2 molecules, and three-body reactions partially take place because of the short mean free path (order of μm) of molecules in viscous flow. The total flow rate is several liters/min under standard conditions and the flow rate ratio of N_2 to NF_3 is 0.5 to 1.0, which is deduced from the overall reaction scheme of



In the experimental aspects, the absolute density of $N_2(A^3\Sigma^+)$,

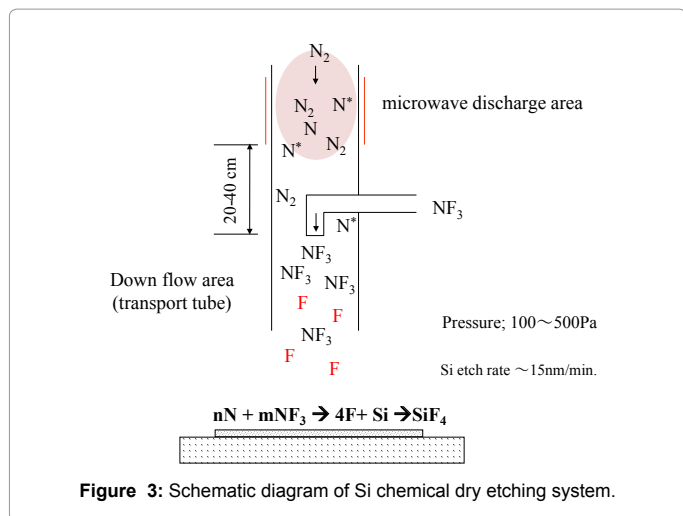


Figure 3: Schematic diagram of Si chemical dry etching system.

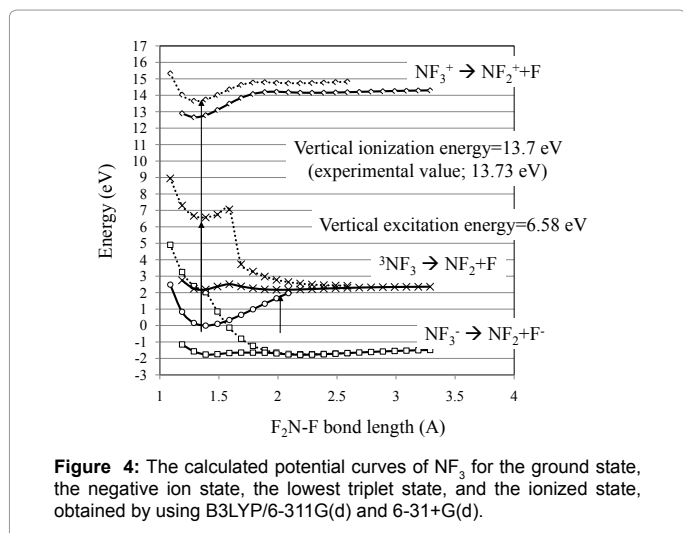


Figure 4: The calculated potential curves of NF_3 for the ground state, the negative ion state, the lowest triplet state, and the ionized state, obtained by using B3LYP/6-311G(d) and 6-31+G(d).

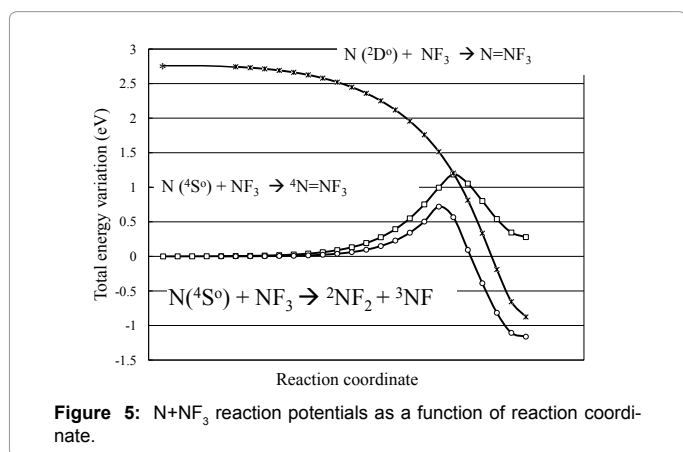


Figure 5: $N+NF_3$ reaction potentials as a function of reaction coordinate.

$N(^4S_0)$ and $N(^2D_0)$ in an inductively coupled nitrogen plasma source were measured by cavity-ringdown and vacuum ultraviolet absorption spectroscopy by Horikawa et al. [27]. It was shown in this report that the densities of the above mentioned three active species at 20 mTorr were almost the same and that the densities of active nitrogen atoms did not change with an increase in the pressure up to 100 mTorr, whereas

the density of $N_2(A^3\Sigma_u^+)$ decreased as the pressure increased. In the theoretical aspect, the rate constant for the $NF_3+N(^4S_0)\rightarrow NF_2+NF$ gas phase reaction was calculated using the transition state theory based on MP2/6-31G(d) of the Gaussian 03 program by Barreto et al. [28], to explain the growth kinetic mechanism of boron nitride films. No other theoretical investigations are found. Therefore, we calculated the $N+NF_x$ ($x=1$ to 3) reactions using a molecular orbital method to clarify the F production mechanism in N_2 downflow plasma and flowing NF_3 .

Figure 4 shows the potential curves of NF_3 for the ground state, the negative ion state and the ionized state with C_{3v} structure, calculated using the B3LYP/6-311G(d). The lowest triplet state was calculated using B3LYP/6-31+G(d) and superimposed on this figure, because the lowest triplet state is a Rydberg state. The calculated energies for these states are good agreements with the experimental ones [29,30]. The calculated vertical transition energy to the lowest triplet state is 6.58 eV. This energy is very close to the $N_2(A^3\Sigma_u^+)$ energy (approximately 7 eV) [31]. This means that the following energy transfer reaction takes place resonantly:

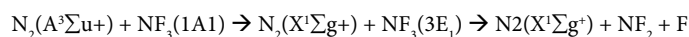
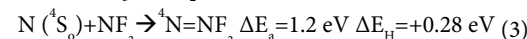


Figure 5 shows $N+NF_3$ reaction potentials as a function of reaction coordinate. The following three reaction schemes are possible:



Where ΔE_a is activation energy (reaction barrier) and ΔE_H is reaction enthalpy, obtained by B3LYP/6-31+G(d). Negative value means exothermic energy. The calculated result for the reaction scheme (2) is almost the same with that obtained by Barreto et al. [28]. The temperature of atomic nitrogen estimated from the spectra taken at 14 cm from the DC discharge area at 100 Pa was estimated as 0.2580 eV for pure N_2 plasma [32]. Therefore, it is considered that the reaction (4) is only possible for $N+NF_3$ reaction. The calculated state energy of $N(^2D_0)$ was approximately 2.75 eV above the ground state energy of $N(^4S_0)$ in B3LYP/6-31+G(d) level, slightly larger than the experimental energy difference of 2.38 eV [31].

The total reaction scheme is summarized and illustrated in Figure 6. The solid line shows the main reaction routes and the dashed line shows the minor reaction routes. Surveying Figure 6 and the aforementioned reaction schemes, it is thought that the electron attachment dissociation can be neglected because the electrons produced in the plasma cannot survive at the NF_3 flowing point (20-40 cm apart from the discharge

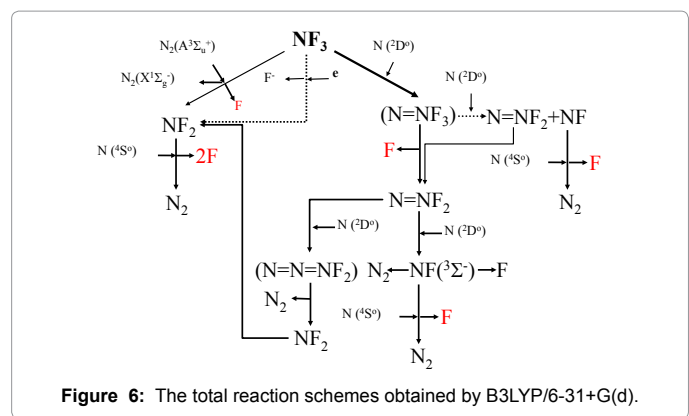


Figure 6: The total reaction schemes obtained by B3LYP/6-31+G(d).

area in the pressure range of 100 to 500 Pa). Similarly, it is deduced that the contribution of $N_2(A^3\Sigma_u^+)$ is not so high, because the density of $N_2(A^3\Sigma_u^+)$ decreases as the pressure increases, whereas the density of $N(^2D^o)$ was not dependent on the pressure (20-100 mTorr), according to the results shown by Horikawa et al. [27]. Therefore, the main reactions should be initiated by $N(^2D^o)$. Then, $NF(^3\Sigma^-)$ and/or NF_2 radicals are produced in the down flow area. NF and NF_2 radicals are very unstable, so these radicals easily react with ground state nitrogen atoms $N(^4S_o)$, proceeding to N_2 molecule and F atom(s). Decreasing the distance between the discharge region and the NF_3 flowing position, Si etch rate increases [25] because the densities of $N_2(A^3\Sigma_u^+)$, and electrons also increase.

CDE Technology without Plasma Source

Chemical dry etching in view of gas-surface chemistry was first studied by Coburn and Winters [14]. In this work, they found that ion irradiation plays a very important role to enhance surface chemical reaction of XeF_2 with Si. This means that bond breaking of Si-Si and dangling bond formation enhances the surface chemical reaction. They also suggested that the purely chemical etch rate by XeF_2 was 0.5-0.7 nm/min at room temperature at the flow rate of $XeF_2=2\times 10^{15}$ mol/s (corresponding to approximately 600 nm/min at 2.7 sccm), without ion irradiation. The surface chemistry of F atoms with Si was further investigated by Flamm et al. [4], using F_2 downflow plasma. They observed the relation between the etch rate and chemiluminescence, emitted from SiF_3^* produced by SiF_2+F reaction near the Si surface, and proposed the surface chemical reaction model that a layer of SiF_2 groups was chemically bound to the Si surface and the rate determinant reaction of impinging F atoms with Si-SiF₂ bonds of the chemisorbed layer controlled the gasification of Si as SiF_2 and higher fluorinated species. Ibbotson et al. [5] studied surface chemical reactions of XeF_2 and F atoms with Si, in pressure range of 0.05 to 2 Torr. They clarified that the chemical reaction of XeF_2 with Si was different from that of F atom with Si. In the case of F atom, the etch rate was fit to a general form of the Arrhenius equation, as a function of substrate temperature, whereas an Arrhenius plot of the XeF_2 etch rate data exhibited a complex behavior. Below 450 K, the etch rate decreased with increasing temperature, between 360 and 450 K, it reached a minimum, and finally at higher temperatures it increased. They concluded that physisorbed and condensed XeF_2 layers contributed to the reaction rate below 450 K temperature region. Similar phenomena were observed

for inter-halogen compounds, such as ClF_3 , BrF_3 and IF_5 with Si [6]. The common properties of these compounds may be having relatively weak bond energy and heavy weight mass. The bond energy of F_2 is also very low (1.8 eV [33]). The low bond energy means very reactive with Si, because Si-F bond energy is very high (approximately 6 eV [34]). The molecules with heavy mass have an inter-molecular force (Van der Waals forces), so the adsorption readily takes place on Si and then bond distortion may take place due to strong Si-F bond energy, resultantly leading to Si etching.

These gases, therefore, are very interesting to etch Si without any plasma source. However, the running cost is too high to respond to requirement of mass production lines.

New CDE System without Plasma Source

A new silicon etching process was innovated by us, using $F_2 + NO \rightarrow F + FNO$ reaction [35], in the pressure region of 100 to 1000 Pa. This technology receives much attention for etching process engineers, in view of the initial and the running costs. The etch rate was comparable with that obtained using XeF_2 chemical dry etching. Arrhenius plot of the etch rate data obtained in the F_2+NO mixing gas exhibited a complex behavior [36], similar to XeF_2 etching. Below 430 K, the etch rate decreased with increasing temperature, it reached a minimum between 430 and 450 K, and finally at higher temperatures it increased. The etch rate as a function of the substrate temperature is shown in Figure 7.

In the feasibility experiments [35,36], A 6 mm (width) \times 15 mm (length) \times 0.53 mm (thickness) Si sample was placed on the ceramic heater, which was covered by the Al foil inserted in the Pyrex[®] tube with the inner diameter of 25 mm and the length of 150 mm. The Si sample was exposed to the gas mixture of NO at a flow rate of 5 sccm (8.5×10^{-3} Pa-m³/s) diluted with Ar at a flow rate of 49.5 sccm (8.4×10^{-2} Pa-m³/s), and Ar/5%- F_2 at a flow rate of 54.5 sccm (9.2×10^{-2} Pa-m³/s). The corresponding F_2 flow rate was 2.7 sccm (4.6×10^{-3} Pa-m³/s). In this study, the temperature on the ceramic heater was adjusted between 27°C and 300°C by the variable autotransformer, while measuring the temperature by the K-type thermocouple placed on top of the ceramic heater under the Si substrate. Pressure in the Pyrex[®] tube was maintained at 600 Pa throughout the process time of 0.5 ~ 5 min. Base pressure of this chamber was maintained at $\sim 10^{-1}$ Pa by the dry pump, so the small amount of H_2O was considered to be remained in the chamber.

Two Si samples were prepared. One was p-type Si (100) sample with the resistivity of ~ 1000 Ω -cm with a 1 μ m-thick SiO_2 mask layer that had 8 μ m \times 8 μ m square patterns. This sample was exposed in NO and F_2 gases for 5 min. for the etch rate and the etched profile analysis. The other was the non-doped Si (100) sample with the resistivity of >3000 Ω -cm for the surface morphology and the surface chemical bonding structure analysis. This sample was cleaned with acetone, ethanol, deionized (DI) water, 13% hydrochloric acid and 49% hydrofluoric (HF) acid for 5 min, followed by rinsing in DI water for <5 s to terminate the Si surface with H. This H-terminated Si sample was exposed to NO and F_2 gases for 0.5 min in the aforementioned process chamber.

Figure 8 shows the representative cross-sectional SEM images of the patterned p-type Si (100) samples placed in NO and F_2 gases, when the Si was heated at 27°C ~ 300°C. We found that the etched Si surface was very rough when the substrate temperature was 27°C, and increasing the temperature up to 70°C, the etch rate decreased and the roughness also decreased. Nanoporous features were observed in the microscopically rough etched profile at this temperature range. When

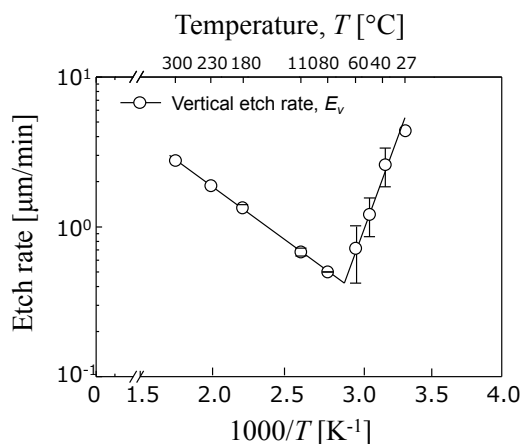


Figure 7: Etch rate was high at room temperature (RT) and decreased with T at $T < 60^\circ C$ and increased with T at $T > 60^\circ C$.

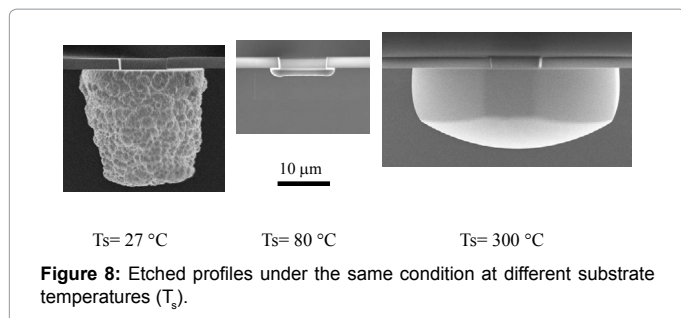


Figure 8: Etched profiles under the same condition at different substrate temperatures (T_s).

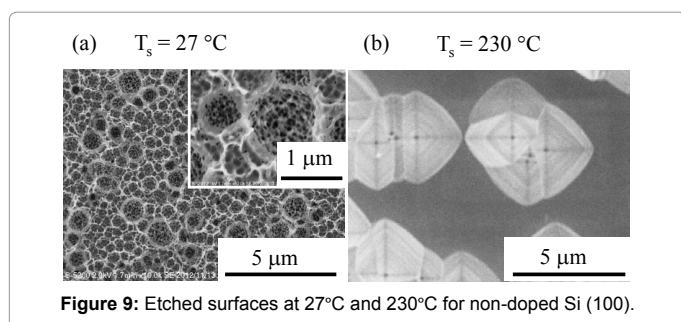


Figure 9: Etched surfaces at 27°C and 230°C for non-doped Si (100).

the Si sample was heated at 60°C ~ 230°C, the etched bottom surface became smooth with the absence of nanoporous features. The etch rate decreased with increase of the temperature up to ~ 70°C and increased again at above 70°C. When the substrate temperature was adjusted at above 230°C, the sidewall of the etched profile became vertical. The crystallographic orientation was observed from these SEM images where the bottom surface was {100} and the sidewall was {110}. Corner undercutting with the exposure of {211} and {411} were also observed at the corner of the etched profile [36].

Thus, morphology of the etched bottom surface and the sidewall surface of the p-doped Si was dramatically changed when the Si was heated at different temperatures. Figure 9 shows the top view of the Si (100) placed in the NO and F₂ gases for 0.5 min. The microscopically rough etched profile were observed, similarly when the Si was chemically dry etched in XeF₂ or ClF₃ gases [5,6]. Previous studies stated that the evolution of the rough surface was due to the chemisorption of not only F but also XeF₂, XeF, ClF₃, Cl₂, Cl that would etch Si differently. The residence time of those molecules on the Si surface was long when the substrate temperature was low. The high Si etch rate at the low temperature in NO and F₂ gases observed in Figure 8 and 9 can be explained by the presence of the chemisorbed F₂, F and others that would promote the etching. In addition to F₂ and F, NO would inhibit the etching by capping the dangling bonds. FNO would act as both a promoter and an inhibitor of the Si etching process by producing and capping the dangling bonds at the surface. These multiple reactions between molecules in the gas phase and the Si surface induced not only microscopically rough etched profile, but also produced complex porous features at low temperature.

The formation of the anisotropic etched profile at 27°C shown in Figure 8a has never been observed when the Si was chemically dry etched in XeF₂ or ClF₃ gases. The formation of this anisotropic etched profile was produced probably due to the chemisorptions of NO, FNO, OH, and (SiF₄)(FNO)₂ at the sidewall. (SiF₄)(FNO)₂ coordinated compound is weakly bounded molecule with intermolecular force of 0.34 eV in B3LYP/6-311+G(d) level. This energy is comparable with that of intermolecular hydrogen bond energy of H₂O-H₂O (approximately

0.2 eV). The boiling point of (SiF₄)(FNO)₂ was reported as 80°C [37]. The contribution of (SiF₄)(FNO)₂ to prevent sidewall etching at a low temperature still needs further investigation by utilizing *in-situ* gas and surface analysis techniques.

In conclusion, Si chemical dry etching was performed in NO and F₂ gases using the exothermic reaction of F₂+NO→F+FNO. The formation of nanoporous features, the initiation of the flat surface and the orientation dependent etched profile were observed by controlling the temperature of the Si substrate between 27°C and 300°C. The chemisorbed F, F₂ and FNO promoted Si etching by forming new dangling bonds, while NO, OH and FNO inhibited etching by terminating the dangling bond at the Si surface at low temperature. The multiple chemical reactions between the molecules in the gas phase and the Si surface occurred at different rates, leading to produce complex nanoporous features in microscopically rough etched profiles. The reduction of F, F₂, FNO and large molecules in the chemisorbed layer decelerated the etch rate at an intermediate temperature. When the substrate temperature was ramped at above 230°C, the Si etching was mainly performed by F, F₂ and FNO at the Si surface, and contribution of NO and the large coordinated compound could be ignored. The crystallographic orientation was evolved and the etch rate increased with the temperature by the increase of the rate constant of F, F₂ and FNO and the Si surface.

Summary

The development of the chemical dry etching technologies is reviewed historically in this literature. The downflow chemical dry etching technology using CF₄/O₂ is now available to fabricate LSI and power devices. The chemical dry etching technology using XeF₂ without plasma is widely used in the field of micro electro-mechanical system (MEMS) fabrication process. The N₂ downflow plasma and NF₃ flow system is considered to be a new damage less process after the poly-Si gate etching, to remove ion damaged layer of 10 nm. The chemical dry etching using ClF₃ gas is considered as a candidate to reduce reflectance of solar cell devices. Thus, the chemical dry etching technologies are selectively used according to adaptable application area.

The chemical dry etching technology in F₂+NO gas mixture is considered as a most promising candidate to be applicable to a wide variety of devices, because of its low initial and running costs and the changeable surface morphology depending on the substrate temperature. The sacrificial layer removal for MEMS devices and the surface texturing for solar cell devices can be carried out at room temperature with the rate of several 1000 nm/min. The damaged layer removal after wafer thinning by the chemical-mechanical polishing (CMP) method for 3 dimensional devices is also capable and anticipated as the most promising technology. This process can be carried out using the ramp technology of the substrate temperature; high rate etching is used in the initial stage and low rate etching with smooth surface is used in the final stage.

References

- Horiike Y, Shibagaki M (1976) A new chemical dry etching. Jpn J Appl Phys suppl 15:13-18.
- Mogab CJ, Adams AC, Flamm DL (1978) Plasma etching of Si and SiO₂-The effect of oxygen additions to CF₄ plasmas. J Appl Phys 49: 3796-3803.
- Flamm DL, Mogab CJ, Sklaver ER (1979) Reaction of fluorine atoms with SiO₂. J Appl Phys 50: 6211-6213.
- Flamm DL, Donnelly VM, Mucha JA (1981) The reaction of fluorine atoms with silicon. J Appl Phys 52: 3633-3639.

5. Ibbotson DE, Flamm DL, Mucha JA, Donnelly VM (1984) Comparison of XeF₂ and F-atom reactions with Si and SiO₂. Appl Phys Lett 44: 1129-1131.
6. Ibbotson DE, Mucha JA, Flamm DL, Cook JM (1984) Plasmaless dry etching of silicon with fluorine-containing compounds. J Appl Phys 56: 2939-2942.
7. Suto S, Hayasaka N, Okano H, Horiike Y (1989) Highly selective etching of Si₃N₄ to SiO₂ employing fluorine and chlorine atoms generated by microwave discharge. J Electrochem Soc 136: 2032-2034.
8. Nishino H, Hayasaka N, Okano H (1993) Damage-free selective etching of Si native oxides using NH₃/NF₃ and SF₆/H₂O down-flow etching. J Appl Phys 74: 1345-1348.
9. Kastenmeier BEE, Matsuo PJ, Oehrlein GS, Langan JG (1999) Silicon etching in NF₃/O₂ remote microwave plasmas. J Vac Sci Technol A 17: 3179.
10. Tsuji M, Okano S, Tanaka A, Nishimura Y (1999) Chemical dry etching of Si substrate in a discharge flow using Ar/CF₄ gas mixtures. Jpn J Appl Phys 38: 6470.
11. Yun YB, Pak SM, Kim DJ, Lee NE, Choi CK, et al. (2008) Thin Solid Films 516: 3549.
12. Coburn JW, Chen M (1980) Optical emission spectroscopy of reactive plasmas: A method for correlating emission intensities to reactive particle density. J Appl Phys 51: 3134-3136.
13. Ninomiya K, Suzuki K, Nishimatsu S, Okada O (1985) Reaction of atomic fluorine with silicon. J Appl Phys 58: 1177-1182.
14. Coburn JW, Winters HF (1979) Ion- and electron-assisted gas-surface chemistry-An important effect in plasma etching. J Appl Phys 50: 3189-3196.
15. Hayashi T, Murai S, Sato F, Kono A, Mizutani N, et al. (2011) Measurement of negative ions generated on the Si etched surface. Jpn J Appl Phys 50: 08KB01-8KB04.
16. Ohchi T, Kobayashi S, Fukasawa M, Kugimiya K, Kinoshita T, et al. (2008) Reducing damage to Si substrates during gate etching processes. Jpn J Appl Phys 47: 5324.
17. Eriguchi K, Ono K (2008) Quantitative and comparative characterizations of plasma process-induced damage in advanced metal-oxide-semiconductor devices. J Phys D 41: 024002.
18. Nakakubo Y, Matsuda A, Fukasawa M, Takao Y, Tatsumi T, et al. (2010) Optical and electrical characterization of hydrogen-plasma-damaged silicon surface structures and its impact on in-line monitoring. Jpn J Appl Phys 49: 08JD02-08JD06.
19. Grubbs RK, George SM (2006) Attenuation of hydrogen radicals traveling under flowing gas conditions through tubes of different materials. J Vac Sci Technol A 24: 486-496.
20. Kikuchi J, Suzuki M, Fujimura S, Yano H (1993) Effects of H₂O on atomic hydrogen generation in hydrogen plasma. Jpn J Appl Phys 32: 3120.
21. Kikuchi J, Iga M, Ogawa H, Fujimura S, Yano H (1994) Native oxide removal on Si surfaces by NF₃-added hydrogen and water vapor plasma downstream treatment. Jpn J Appl Phys 33: 2207-2211.
22. Inoue H, Higuchi Y, Suu K (2011) Private communication.
23. Hayashi T, Ishikawa K, Sekine M, Hori M, Kono A, et al. (2012) Quantum chemical investigation for chemical dry etching of SiO₂ by flowing NF₃ into H₂ downflow plasma. Jpn J Appl Phys 51: 016201.
24. Verrcke G, Schaekers M, Verstraete K, Arnauts S, Heyns MM, et al. (2000) J Electrochem Soc. 147: 1499.
25. Tajima Y, Takahashi S (2011) Japan Patent JP2010165954 and private communication.
26. Hayashi T, Ishikawa K, Sekine M, Hori M, Kono A, et al. (2012) Quantum Chemical Investigation of Si Chemical Dry Etching by Flowing NF₃ into N₂ Downflow Plasma. Jpn J Appl Phys 51: 026505.
27. Horikawa Y, Kurihara K, Sasaki K (2010) Absolute Densities of N₂A₃Σ_u⁺, N(⁴So), and N(²Do) in an Inductively Coupled Nitrogen Plasma Source. Jpn J Appl Phys 49: 026101.
28. Barreto PRP, Vilela AFA, Gargano R, Ramalho SS, Salviano LR (2006) NF₃+N=NF₂+NF rate constant calculated using TST with simple tunneling correction J Mol Struct: Theochem 769: 201-205.
29. Bassett PJ, Lloyd DR (1970) Chem Phys Lett 6: 166.
30. Kalyuzhnaya AG, Ryabtsev AV, Shchedrin AI (2008) Electron energy distribution function in a hollow-cathode glow discharge in mixtures of nitrogen with electronegative gases. Tech Phys 48: 38-42.
31. Steinfeld JI (1985) Molecules and radiation: An introduction to modern molecular spectroscopy. (2nd Ed.), New York, USA 106.
32. Suraj KS, Bharathi P, Prahlad V, Mukherjee S (2007) Near cathode optical emission spectroscopy in N₂-H₂ glow discharge plasma. Surf Coat Technol 202: 301-309.
33. Jones WE, Skolnik EG (1976) Reactions of fluorine atoms. Chem Rev 76: 563-592.
34. Fisher ER, Kickel BL, Armentrout PB (1993) Collision-induced dissociation and charge-transfer reactions of SiFx⁺ (x=1-4). Thermochemistry of SiFx and SiFx⁺. J Phys Chem 97: 10204-10210.
35. Tajima S, Hayashi T, Ishikawa K, Sekine M, Hori M (2013) Room-temperature Si etching in NO/F₂ gases and the investigation of surface reaction mechanisms. J Phys Chem C 117: 5118-5125.
36. Tajima S, Hayashi T, Ishikawa K, Sekine M, Hori M (2013) 5th Intern. Symp. Adv. Plasma Sci. Appl. Nitrides and Nanomaterials (ISPLASMA) 187.
37. Kigoshi A (1975) Differential scanning calorimetry study of complex fluorides of zirconium, tin, vanadium, silicon, antimony, molybdenum and tellurium. Thermochemica Acta 12: 179-187.